# A quantitative model of the generation of $N^{\varepsilon}$-(carboxymethyl)lysine in the Maillard reaction between collagen and glucose

António E. N. FERREIRA*†[1], Ana M. J. PONCES FREIRE* and Eberhard O. VOIT†‡

*Departamento de Química e Bioquímica, Faculdade de Ciências da Universidade de Lisboa, Bloco C8, Campo Grande, 1749-016 Lisboa, Portugal, †Department of Biometry and Epidemiology, Medical University of South Carolina, Charleston, SC 29425, U.S.A., and ‡Department of Biochemistry and Molecular Biology, Medical University of South Carolina, Charleston, SC 29425, U.S.A.

The Maillard reaction between reducing sugars and amino groups of biomolecules generates complex structures known as AGEs (advanced glycation endproducts). These have been linked to protein modifications found during aging, diabetes and various amyloidoses. To investigate the contribution of alternative routes to the formation of AGEs, we developed a mathematical model that describes the generation of CML [$N^{\varepsilon}$-(carboxymethyl)lysine] in the Maillard reaction between glucose and collagen. Parameter values were obtained by fitting published data from kinetic experiments of Amadori compound decomposition and glycoxidation of collagen by glucose. These raw parameter values were subsequently fine-tuned with adjustment factors that were deduced from dynamic experiments taking into account the glucose and phosphate buffer concentrations. The fine-tuned model was used to assess the relative contributions of the reaction between glyoxal and lysine, the Namiki pathway, and Amadori compound degradation to the generation of CML. The model suggests that the glyoxal route dominates, except at low phosphate and high glucose concentrations. The contribution of Amadori oxidation is generally the least significant at low glucose concentrations. Simulations of the inhibition of CML generation by aminoguanidine show that this compound effectively blocks the glyoxal route at low glucose concentrations (5 mM). Model results are compared with literature estimates of the contributions to CML generation by the three pathways. The significance of the dominance of the glyoxal route is discussed in the context of possible natural defensive mechanisms and pharmacological interventions with the goal of inhibiting the Maillard reaction *in vivo*.

Key words: advanced glycation endproduct, Amadori product, dynamical model, glyoxal, Maillard reaction, Namiki pathway.

## INTRODUCTION

AGEs (advanced glycation endproducts) are post-translational protein modifications that result from a network of reactions between basic amino acid residues and carbohydrates or reactive carbonyls. The ensemble of these reactions, collectively termed the 'Maillard reaction', is perceived to be a slow but complex process that occurs spontaneously in living organisms without the action of specific enzymes.

The presence of AGEs has been correlated with age in several species [1] and with the severity of some human pathologies such as diabetes [2,3] and Alzheimer's disease [4]. In some cases, a specific mechanistic role of these protein modifications was hypothesized to cause clinical complications associated with these pathologies (for recent reviews, see [5–7]). For instance, it has been proposed that at the early onset of Alzheimer's disease the formation of glycation end products could be a key factor in the aggregation of the Tau protein in paired helical filaments and in the abnormal processing of the amyloid precursor protein that is characteristically found in Alzheimer's patients [4]. While there is still a lack of clear evidence associating causality with protein modifications, AGE levels are usually considered to be good biochemical markers of the progression of these pathologies. As a consequence, research has been directed toward the identification of the mechanisms and kinetics of the Maillard reaction *in vivo* in the hope of collating sufficient information to support the development of pharmacological interventions that would inhibit some of the crucial steps of AGE accumulation and degradation. Examples of such inhibitors of the Maillard reaction are aminoguanidine [8], tenilsetam [9], pyridoxamide [10] and metformin [11].

Among the numerous AGEs that have been described, CML [$N^{\varepsilon}$-(carboxymethyl)lysine] appears to be the best-characterized. CML levels are usually found to be higher than most other AGEs, and correlate well with overall AGE measures in proteins [12,13]. Furthermore, CML is one of the major epitopes recognized by antibodies raised against AGE modified proteins [14].

CML can be formed by three concurrent mechanisms *in vivo* (Scheme 1). In the classical glycoxidation pathway, the Schiff base, which results from the reaction between glucose and lysine, rearranges into a ketoamine, the Amadori product, which is then oxidatively fragmented to give CML, among other products [15]. In the 'autoxidative glycosylation' pathway, CML is formed by the reaction between lysine and glyoxal, the latter of which results from metal-catalysed autoxidation of glucose [16,17]. In a third mechanism, called the Namiki pathway, two carbon fragments including free glyoxal are formed by fragmentation and oxidation of the Schiff base, and can subsequently form CML [18].

Attempts to establish the relative contribution of each of these pathways to the generation of CML have so far been inconclusive or even contradictory to some extent. Glomb and Monnier [18] suggested that the oxidation of the Amadori product accounts for most of the CML formed in a model system of glucose and amino-blocked lysine. Their conclusion was based on the observation that the formation of CML is only partially inhibited by the addition of aminoguanidine, a compound known to trap glyoxal. The authors estimated the contribution of the autoxidative pathway to be negligible. By contrast, Wells-Knecht and co-workers [19]

Abbreviations used: AGE, advanced glycation endproduct; CML, $N^{\varepsilon}$-(carboxymethyl)lysine.

[1] To whom correspondence should be addressed (e-mail aeferreira@fc.ul.pt).

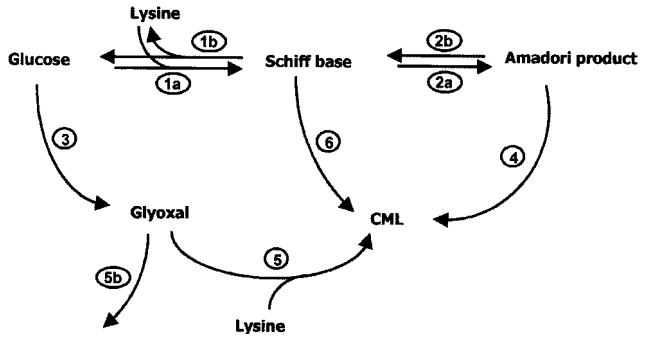


**Scheme 1 Simplified reaction network of the early steps of the Maillard reaction and CML formation**

See Table 1 for a description of the reactions.

found in a model system of labelled glucose and unlabelled preglycated collagen that most of the CML originated from glucose autoxidation or the Namiki pathway and that fragmentation of the Amadori compound was partially inhibited at high glucose concentrations. They determined the contribution of the Amadori compound to CML formation to be quantitatively similar to that of the Namiki and autoxidation pathways only at low glucose and phosphate buffer concentrations.

The assessment of the relative contributions of each of these pathways is far from being solely an academic question. It is crucial for elucidating potential physiological defence systems against the Maillard reaction, as well as for guiding the development of drugs that target the reduction of AGE accumulation *in vivo*. As a first step in this direction, Khalifah and co-workers [10] classified such inhibitor drugs of the Maillard reaction according to their effect on each of the concurrent pathways [10].

The primary goal of this paper is to address the question of the relative importance of the different pathways that lead to the generation of CML. This is accomplished by constructing a mathematical model of the early steps of the Maillard reaction in systems of glucose and collagen. As a quantitative description of these reactions, the model provides a convenient tool for making semi-quantitative predictions about the relative contributions and their dependence on key kinetic parameters.

## MATERIALS AND METHODS

### General strategies

The development of the model follows a two-phase process. In the first phase, we develop a preliminary model and implement it with kinetic parameters collected or deduced from experimental results published in the literature about each of the different local processes that make up the network of reactions considered in the model. These parameter values have reference character only, because they are taken from different tissues under various conditions, are based on assumptions that cannot always be tested and, due to their strict association with only one reaction step each, do not fully account for the connectivity and integrity of the system of pathways that ultimately lead to CML.

The reference description is refined in the second phase by adjusting the raw parameters to fit several published data sets describing the dynamic behaviour of relevant metabolites. These data show the temporal development of CML and some intermediates in reaction mixtures of glucose and collagen under differently conditions. Systematic comparisons between experimental and simulated data in this phase allow the sequential optimization of all parameter values of the model, one at a time.

Although the Maillard reaction has been known for almost a century [20], many details of the governing chemical mechanisms are quantitatively ill-characterized. The strategy for dealing with this situation is to combine unknown or poorly characterized processes into aggregate reactions. It is known that these can be represented with mathematical rigor and validity as power-law rate functions. The power-law functions are used in the present study to assemble a dynamic model in the form of a generalized mass-action model within the tenets of Biochemical Systems Theory [21–24]. Simulations with this model were performed with the software package PLAS (http://correio.cc.fc.ul.pt/~aenf/plas.html) [23].

### Reference model

The processes considered in the preliminary reference model are shown in Scheme 1 and the kinetic details of individual processes in Table 1 (reactions 1–6). 'Lysine' refers collectively to the total amount of lysine residues available for glycation in a given protein.

The following comments may elucidate the rationale for some of the reactions in the reference model; reactions not discussed are directly derived from the references in Table 1.

#### Schiff base formation and reverse reaction (reactions 1a and 1b)

These processes are modelled by elemental mass-action kinetics. A variety of values for the rate constants for human serum albumin [25], haemoglobin [26] and RNase [27] are available in the literature for different conditions.

Values for the rate constant of reaction 1a differ by more than one order of magnitude, which is in part due to differences in

**Table 1 Reference kinetics for the reactions in Schemes 1 and 2**

Ox has a value of either 0 or 1, and models the absence or presence of oxidative conditions.

| Reaction no. | Description | Rate law | Reference |
|---|---|---|---|
| 1a | Schiff base formation, forward | $p_1$ 0.09 $M^{-1} \cdot h^{-1}$ [Glu] [Lys] | See text and Tables 2 and 3 |
| 1b | Schiff base formation, reverse | 0.36 $h^{-1}$ [Schiff] | See text and Tables 2 and 3 |
| 2a | Amadori rearrangement | $p_2$ 0.033 $h^{-1}$ [Schiff] | [32] |
| 2b | Amadori rearrangement, reversal | $p_2$ 0.0012 $h^{-1}$ [Amadori] | [29] and see text |
| 3 | Glucose autoxidation | $p_3$ $7.92 \times 10^{-7}$ $M^{-1} \cdot h^{-1}$ ([Glu]/0.25 M)$^{0.36}$ Ox | [17] and see text |
| 4 | Amadori oxidative cleavage | $p_4$ 0.000086 $h^{-1}$ [Amadori] Ox | [19] |
| 5 | CML from Lys and Glyoxal | $p_5$ 0.019 $M^{-1} \cdot h^{-1}$ [Glyoxal] [Lys] Ox | [17] |
| 5b | Glyoxal decomposition | 0.0017 $h^{-1}$ [Glyoxal] | [17] |
| 6 | Namiki pathway | $p_6$ $7.92 \times 10^{-7}$ $M^{-1} \cdot h^{-1}$ ([Schiff]/0.25 M)$^{0.36}$ Ox | See text |
| 7 | Other Schiff base reactions | $p_7$ $7.92 \times 10^{-7}$ $M^{-1} \cdot h^{-1}$ ([Schiff]/0.25 M)$^{0.36}$ Ox | See text |

**Table 2 Kinetic constants for reactions 1a and 1b**

$K_f$ is the equilibrium constant. TAPSO buffer contains 3-(*N*-tris(hydroxymethyl)-methylamino)-2-hydroxypropanesulphonic acid.

| Protein | $k_{1a}$ ($M^{-1} \cdot h^{-1}$) | $k_{1b}$ ($h^{-1}$) | $K_f$ ($M^{-1}$) | Reference |
|---|---|---|---|---|
| Human serum albumin | 1.5 | 0.39 | 3.9 | [25] |
| Haemoglobin | 0.9 | 0.33 | 2.7 | [26] |
| RNase (phosphate buffer) | – | – | 1.3 | [27] |
| RNase (Mops buffer) | – | – | 1.9 | |
| RNase (TAPSO buffer) | – | – | 1.6 | |

**Table 3 Kinetic constants for reaction 1a, adjusted by number of reactive lysine residues**

| Protein | Number of residues glycated | $k_{1a}$ ($M^{-1} \cdot h^{-1}$; per lysine residue) | Reference |
|---|---|---|---|
| Human serum albumin | 10 Lys + 1 $\alpha NH_2$ | 0.14 | [36] |
| Haemoglobin | 10 – 14 Lys | 0.06–0.09 | [26] |
| RNase | 4 Lys + 1 $\alpha NH_2$ | 0.09 | [27] |

the number of lysine residues per substrate molecule (Table 2). To overcome this issue, we determined a suitable parameter value by dividing the reported rate constants by the number of lysine residues that had been found to be glycated in each protein (Table 3). With this adjustment, the values agreed within one order of magnitude. The rate constant for RNase in phosphate buffer was considered to be the reference value [27].

Values for reaction 1b were found to be consistent, and we adopted their average as the reference value.

### Reversal of Amadori rearrangement (reaction 2b)

The kinetics of this reaction can be deduced from studies of the degradation of model Amadori products [18,19,28,29]. It is clear from these studies that, under antioxidative conditions, Amadori product degradation is the result of several concurrent reactions, in addition to the reversal of Amadori rearrangement followed by Schiff base hydrolysis. Although these two processes are expected to form hexoses and free lysine residues only, pentoses and tetroses were also found as products in these model systems, the latter at a rate comparable to those for hexoses [29]. The reference value for the rate constant was computed from the initial rate of formation of hexoses (which account for more than 90 % of the sugars produced) under antioxidative conditions in the experiments of Zyzak and collaborators [29]. This value was based on the assumption that the most feasible mechanisms for the generation of free hexoses in Amadori product degradation experiments comprise the reversal of Amadori rearrangement as a first step and that the subsequent Schiff base hydrolysis is not rate limiting. We considered that the origin of $C_4$ compounds in those experiments derive from the degradation of the Schiff base, as proposed in the literature [18,30], and that the rate of these reactions is low compared with the hydrolysis of the Schiff base.

### Formation and degradation of glyoxal during glucose autoxidation (reaction 3)

Autoxidation processes are complex by nature, and even mechanisms describing the oxidation of simple sugars are confounded by free radicals and metal-catalysed autocatalytic reactions [31]. In our model the autoxidation reactions of glucose are lumped into one process and represented with power-law kinetics. This aggregation of reactions is discussed in the Conclusions section.

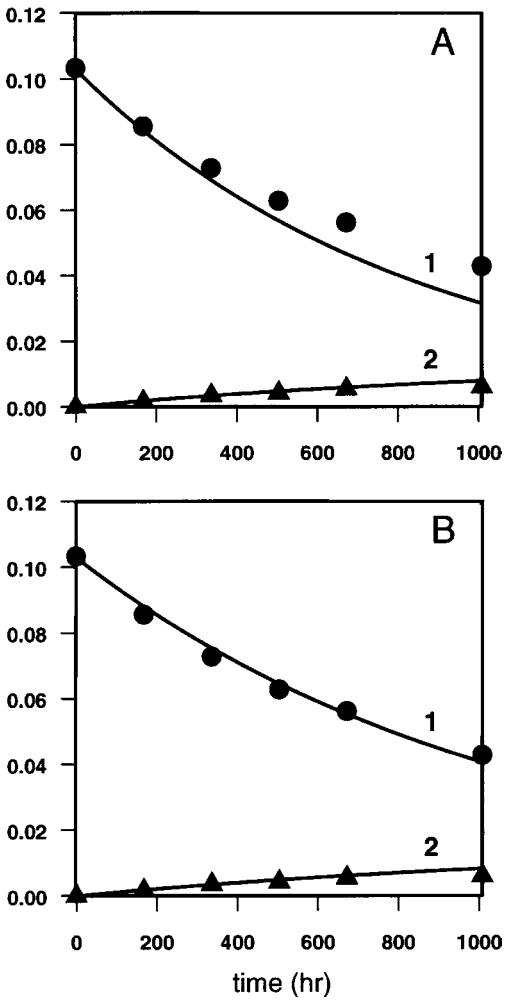


**Figure 1 Time-course data for Amadori product decomposition under oxidative conditions**

Experimental (symbols) and simulated (lines) variables are Amadori (●, line 1) and CML (▲, line 2). Variables are expressed as fraction of total lysine. Experimental data are from [19]. (**A**) Reference model (parameter values from Table 1). (**B**) Reference model adjusted with $p_2 = 0.75$.

Wells-Knecht and others [17] showed that glucose autoxidation results in the generation of the oxoaldehyde glyoxal and the pentose arabinose, and that glyoxal degrades at a rate comparable with its rate of formation. In the work of these authors, the formation of glyoxal seems to deviate from elemental mass-action kinetics, which suggests the use of power-law kinetics as the simplest and most straightforward generalization. The rate constant was calculated from the data for the experiments with the largest glucose concentration (250 mM). The kinetic order was found through one-dimensional optimization, in which we minimized the sum of squared deviations between the experimental glyoxal concentrations and those predicted by the simulation of the two-reaction system of glyoxal formation and degradation.

### Formation of CML from Amadori product (reaction 4)

The reference value was computed as the initial rate of CML formation in experiments of Wells-Knecht and collaborators [19] (Figure 1B). The use of the initial rate assumes that other pathways

of CML generation must occur subsequent to the reversal of the Amadori rearrangement (which has a rate comparable with the oxidation) and will not be significant at very early stages in Amadori product degradation experiments.

### Namiki pathway (reaction 6)

Glomb and Monnier [18] demonstrated the importance of the generation of CML from the Schiff base and proposed mechanisms based on the oxidation of the $C_2$ compounds glyoxal and glycoaldehyde and their lysine Schiff bases as intermediates in the process. These processes are referred to as the Namiki pathway. The reference kinetics are based on the assumption that the mechanism is similar to an amine-mediated autoxidation of the carbohydrate. Under this assumption, an analogous power-law rate law is assigned to this pathway as a default (Table 1, reaction 6).

### Lysine concentration

The total lysine residue concentration was estimated from the collagen concentration used in the validating experiments that we considered in this work and from an average ratio of lysine mass to total mass of collagen based on sequences published by Swiss-Prot (http://us.expasy.org/sprot/sprot-top.html). Again, this is a preliminary reference value that does not take into account the availability of the residues for glycation and CML generation. The adjustment of the rate constant for the forward reaction of Schiff base formation (reaction 1a) will account not only for potential catalytic effects of pH and the nature of buffer used but will also represent the average availability of the lysine residues in collagen for reaction with glucose.

### Oxidative milieu

The parameter 'Ox', with a value of either 0 or 1, models the absence and presence of oxidative conditions.

## Modifications of the reference model

The estimations in the previous section focused on one reaction at a time, without regard for other reactions in the system. In this section the second phase of model development is discussed, where dynamic data are analysed to fine-tune the reference parameter values, as given in Table 1. The published results used for this purpose were obtained from *in vitro* experiments with a glucose-collagen system [12,19]. The experiments were performed in the same laboratory, with the same protein, and under comparable experimental conditions. Given the general uncertainties surrounding the effects of different conditions, this consistency is very valuable for modelling purposes. The choice of data on the collagen-glucose system is also of particular relevance because collagen is a long-lived protein that is believed to be strongly affected by the Maillard reaction *in vivo*.

Some of the data express time-course information, while others express levels of different variables at a certain time point as a function of different concentrations of glucose and the phosphate buffer, and in the presence or absence of oxidative conditions. Therefore, these data relate to the global behaviour of the system as opposed to the parameter values in Table 1, which are based on local information for each reaction or process.

In order to make the effects of the adjustments as translucent as possible, the original parameter values are retained but multiplied with non-dimensional adjustment factors $p_1$–$p_6$ (Table 1) that provide an immediate impression of how much the reference and the adjusted parameter values differ.

### Data set 1: oxidative decomposition of Amadori product of collagen-lysine and glucose

Parameters $p_1$–$p_6$ were investigated with respect to their influence on the fit of the model to time-series measurements of Amadori compound and CML [19]. Only two parameters had a significant effect. Parameter $p_2$ greatly influenced the Amadori rearrangement in reactions 2a and 2b, and $p_4$ strongly affected CML in reaction 4. Quantitatively diagnosing these effects, we found that $p_2$ should have a value of about 0.75, whereas the reference value of $p_4$ was sufficiently accurate already. Figure 1(A) shows the results using the baseline parameters and Figure 1(B) shows the results with the modification in $p_2$.

### Data set 2: formation of Amadori product of collagen-lysine and glucose under antioxidative conditions

With $p_2$ adjusted and $p_4$ retained at the reference value, the only other parameter with potentially important influence on the concentration of the Amadori product is $p_1$, because $p_3$, $p_4$ and $p_6$ are set to zero under antioxidative conditions. An adjustment in $p_1$ can be employed to correct the concentration of Amadori product at some late time point. One should recall here that the parameters are defined on a time scale of hours (see Table 1), but that AGE formation has implications on a much slower time scale, stretching to that of a human life. It is therefore not surprising that investigators studying long-term accumulation of AGEs report values with great experimental variability. We will analyse these results at different time scales elsewhere. For our analysis here, we use a level of Amadori product at 5 weeks under antioxidative conditions, as reported by [19] (Table 1), and adjust $p_1$ to 0.115. Results of this adjustment are shown in Figure 2(A) (see below).

### Data set 3: differences between the formation of Amadori compound and CML under oxidative and antioxidative conditions

Fu and co-workers [12] studied the glycoxidation of collagen by glucose and observed a significant difference in the formation of both Amadori compound and CML under oxidative and antioxidative conditions. This result is expected for CML since the formation of this AGE requires oxygen. However, the decrease in the formation of Amadori product under oxidative conditions provides new information that can be used to adjust the other parameters in the model. The reported data consist of time-series profiles for the two variables and for up to five weeks. They indicate that the formation of CML is approximately linear with time under oxidative conditions and essentially absent under anti-oxidative conditions. The accumulation of Amadori product is hyperbolic and saturates at different levels, depending on oxidative state and conditions.

Figure 2 shows model results obtained for various parameter adjustments. In Figure 2(A), parameters $p_1$ and $p_2$ are modified according to data sets 1 and 2, as discussed above. Retaining the remaining values at their reference levels leads to predicted accumulations of Amadori compound and CML that are clearly not optimal. We could theoretically adjust $p_5$, but fixed its value as 1, since this parameter refers to a reaction that is very well characterized, which lends credence to the originally chosen reference value.

Simulations showed that variations in $p_6$ contributed to an approximately linear accumulation of CML with time, whereas $p_3$ resulted in a slightly convex CML accumulation. However,

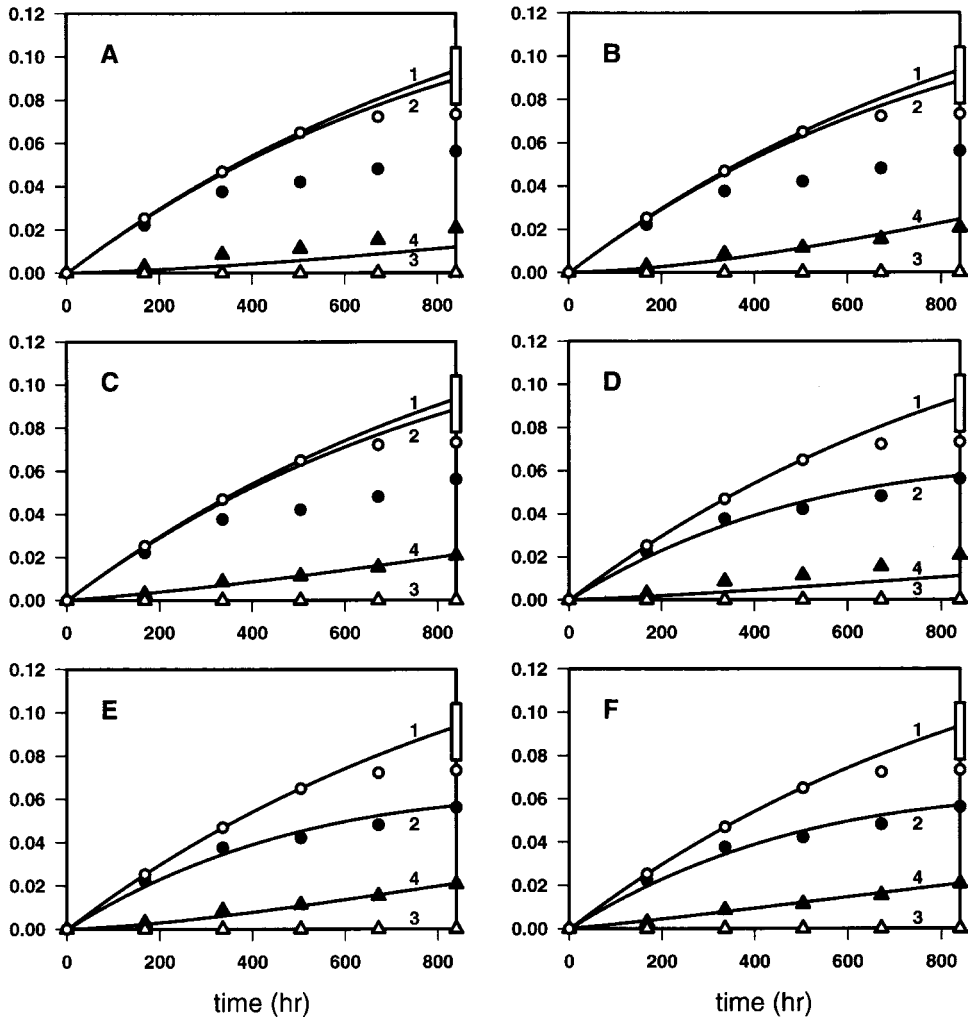


**Figure 2 Time-course data for glycoxidation experiments**

Experimental (symbols) and simulated (lines) variables are (○, line 1) Amadori, antioxidative conditions; (●, line 2) Amadori, oxidative conditions; (△, line 3) CML, antioxidative conditions; and (▲, line 4) CML, oxidative conditions. Variables are expressed as a fraction of total lysine. Experimental data are from [12]. Parameter values: (**A**) baseline model (Scheme 1) with $p_1 = 0.115$, $p_2 = 0.75$; (**B**) baseline model (Scheme 1) with $p_1 = 0.115$, $p_2 = 0.75$, $p_3 = 5$; (**C**) baseline model (Scheme 1) with $p_1 = 0.115$, $p_2 = 0.75$, $p_6 = 2.7$; (**D**) extended model (Scheme 2) with $p_1 = 0.115$, $p_2 = 0.75$, $p_7 = 60$, $f_L = 0.05$, $f_G = 0.1$; (**E**) extended model (Scheme 2) with $p_1 = 0.115$, $p_2 = 0.75$, $p_7 = 60$, $f_L = 0.05$, $f_G = 0.1$, $p_3 = 5$; (**F**) extended model (Scheme 2) with $p_1 = 0.115$, $p_2 = 0.75$, $p_7 = 60$, $f_L = 0.05$, $f_G = 0.1$, $p_6 = 2.7$. Other parameters are $p_3 = p_4 = p_5 = p_6 = 1$, except where indicated. The bar at the top right of each panel indicates a range of values for the yield of Amadori product at 5 weeks under antioxidative conditions as reported in another paper from the same research group [19]; it illustrates the high variability in the determination of this variable in glycation experiments.

none of the one-parameter adjustments was able to capture simultaneously the observed decrease in Amadori under oxidative conditions (Figures 2B and 2C). This suggested that the model had to be extended to include other reactions that would validly represent both variables.

One way to achieve this goal was to include a reaction initiating at the Schiff base, but leading to the generation of products other than CML. The existence of reactions of this type of was proposed in some of the mechanisms for the generation of AGEs [18,30]. Thus we included in the model an additional process of lysine consumption, which lowers the concentrations of both Schiff base and Amadori product under oxidative conditions as compared with antioxidative conditions. The details of this step are shown in Table 1 as reaction 7. The model scheme including the new reaction is shown in Scheme 2.

So far, we have not specified a particular product for this reaction, but the possible regeneration of free lysine residues has to be taken into account. For that purpose, we modify the differential

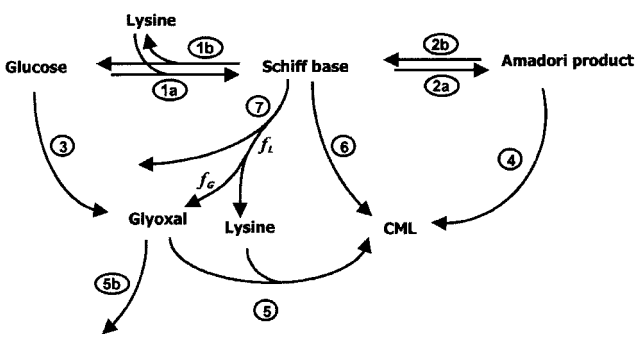


**Scheme 2 Extended reaction network of the early steps of the Maillard reaction and CML formation, including Schiff base reactions other than the Namiki pathway**

See Table 1 for a description of the reactions.

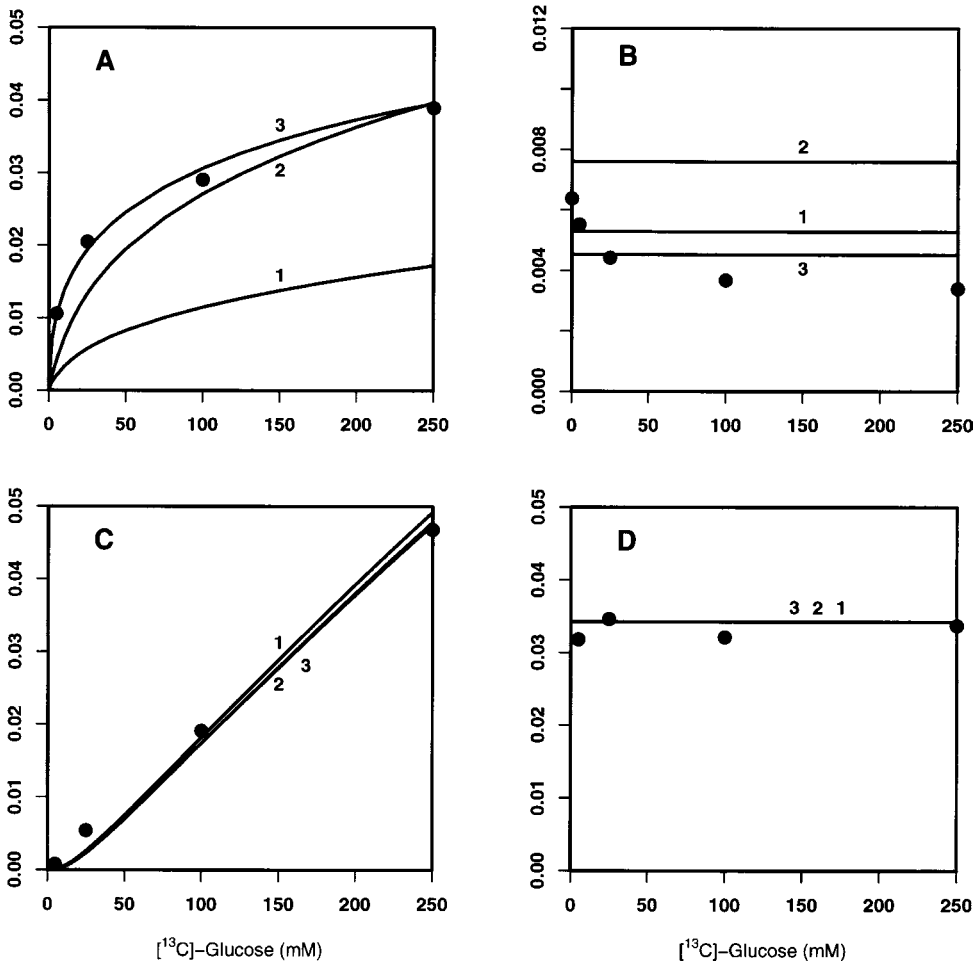


**Figure 3 Double isotope glycoxidation experiments, effect of initial glucose concentration**

Experimental (symbols) and simulated (lines) values at 5 weeks in experiments starting with [$^{13}$C]glucose and [$^{12}$C]Amadori product as 0.095 of total lysine. Variables, expressed as fraction of total lysine, are (**A**) [$^{13}$C]CML, (**B**) [$^{12}$C]CML, (**C**) [$^{13}$C]Amadori and (**D**) [$^{12}$C]Amadori. Phosphate concentration was 200 mM. Parameters are: 1, $p_3 = 1$, $p_6 = 2.7$; 2, $p_3 = 1$, $p_6 = 6.5$; 3, $p_3 = 14$, $p_6 = 1$. Other parameters are as in Figure 2(D). Note the different scale of the *y* axis in the top right-hand panel.

equation for lysine by multiplying the flux through this reaction by a factor $f_L < 1$, reflecting the presence of possible Schiff base decomposition reactions that generate lysine and products other than glucose. According to Glomb and Monnier [18], these Schiff base degradation processes include the release of free glyoxal. Therefore we also considered the formation of glyoxal in the flux that regenerates lysine from the Schiff base and included a fraction $f_G < 1$ of this flux in the differential equation for glyoxal.

These amendments made it possible to determine parameters $p_3, p_6, p_7, f_L$ and $f_G$ (Scheme 2) that resulted in a good model fit of the experimental data for Amadori product under both oxidative and antioxidative conditions (Figure 2D) and for CML (Figures 2E and 2F). At this point there is no clear evidence supporting either modifications in Figures 2(E) or 2(F) over the others.

It is noted that other reactions of Amadori decomposition do exist [29] but were not considered here. One is cleavage of Amadori compound, forming carboxylactoyllysine, which has a much lower rate than CML generation and was considered to be negligible (zero) in the model. Another is the non-oxidative rearrangement of Amadori product into the oxoaldehyde 3-deoxyglucosone. Again the rate of this reaction is probably low compared with CML generation. Furthermore, it has been observed *in vitro* that the decomposition of Amadori product may lead not only to $C_6$ sugars, but also to $C_5$ and $C_4$ fragments [29]. We assumed in the model that the only significant source of $C_4$ fragments (which are formed at a rate comparable to $C_6$ compounds) during the Amadori product decomposition follows from the reversal of the Amadori rearrangement and Schiff base decomposition, as suggested in the mechanisms of the generation of glyoxal and glycolaldehyde in the Namiki pathway [18,30]. Nevertheless, one cannot exclude that the secondary reactions could become noticeable for higher concentrations of Amadori product and would constitute an additional sink.

### Data set 4: distribution of carbon isotopes in double labelling experiments

Wells-Knecht et al. [19] published results of an experiment where the initial reagents were glucose labelled with $^{13}$C and Amadori product labelled with $^{12}$C. The data comprise concentrations of [$^{13}$C]Amadori, [$^{12}$C]Amadori, [$^{13}$C]CML and [$^{12}$C]CML after 5 weeks of reaction under oxidative conditions as a function of [$^{13}$C]glucose concentration.

This type of data is very informative and provides another opportunity to adjust the parameters of the model. As seen in Figure 3, the results for each of the variables, as predicted by the

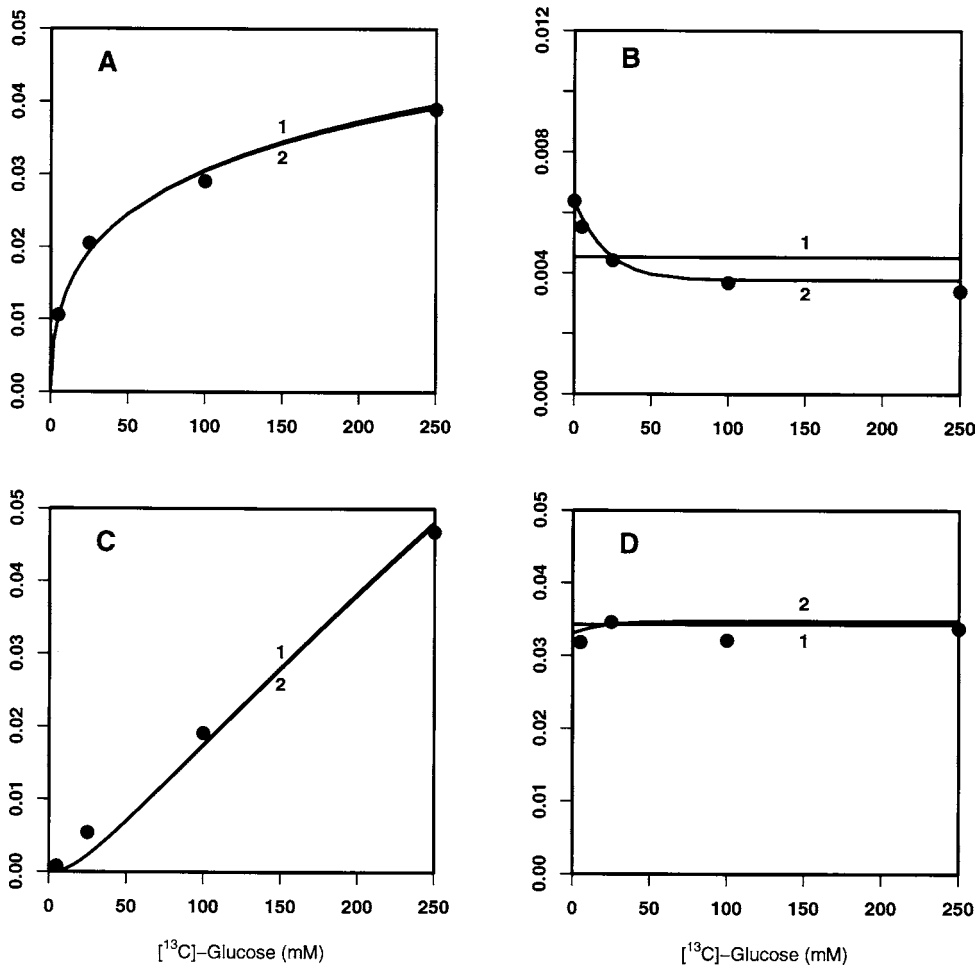


**Figure 4 Double isotope glycoxidation experiments, effect of initial glucose concentration**

Experimental (symbols) and simulated (lines) values at 5 weeks in experiments starting with [$^{13}$C]glucose and [$^{12}$C]Amadori product as 0.095 of total lysine. Variables, expressed as fraction of total lysine, are (**A**) [$^{13}$C]CML, (**B**) [$^{12}$C]CML, (**C**) [$^{13}$C]Amadori and (**D**) [$^{12}$C]Amadori. Phosphate concentration was 200 mM. Parameters are: lines 1, $p_3 = 14$, $p_6 = 1$; lines 2, $p_3 = 14$, $p_6 = 1$, $p_4 = 0.8$; reaction 4 was adjusted as in Table 4. Other parameters are as in Figure 2(D).

model with the parameter values in Figure 2(F), underestimate [$^{13}$C]CML, but the other variables are reasonably close to the experimental data. It is interesting to note that the reported [$^{13}$C]CML values are about twice as high as those obtained in similar experiments by the same laboratory [12], which again attests to the extreme variability in available experimental data on the Maillard reaction.

The parameters $p_3$ and $p_6$ are candidates for adjustment with the possibility of an improved representation of [$^{13}$C]CML. Only the modification of $p_3$ resulted in a good fit, as shown in Figure 3.

Another adjustment of parameter values was suggested by the observation that the [$^{12}$C]glucose concentration at 5 weeks decreases with the initial [$^{13}$C]glucose concentration, a behaviour not predicted by the model with the settings specified so far. An adjustment factor $p_4$, depending on glucose concentration, was introduced in the model to account for slight glucose inhibition of the oxidative fragmentation of the Amadori product into CML (Table 4). Results are shown in Figure 4.

Similar adjustments, defined as functions of the phosphate buffer concentration, were also introduced in the model (Table 4) to account for the significant catalytic effect of anions in the buffer, as clearly demonstrated earlier in various *in vitro* model systems [29,32]. A comparison of the experimental and predicted values of the four variables for different [$^{13}$C]glucose and phosphate buffer concentrations is shown in Figures 4 and 5. Given the general good agreement between model predictions and experimental data, the fine-tuned model, summarized in Table 5, was considered to be sufficiently adequate to serve as a basis for further explorations.

**Table 4 Adjustment factors taking into account glucose and phosphate concentrations**

| Reactions affected | Adjustment factor |
|---|---|
| 2 | $0.57 + 0.43\ ([\text{phosphate}]/0.2\ \text{M})^4$ |
| 4 | $([\text{Phosphate}]/0.2\ \text{M})^{0.6}\ (1 + 0.8764\ \{(0.25\ \text{M} - [\text{Glu}])/0.25\ \text{M}\}^{12})$ |
| 3, 6, 7 | $([\text{Phosphates}]/0.2\ \text{M})^{1.1}$ |

## RESULTS AND DISCUSSION

### Importance of different pathways for the accumulation of CML

An important question about the Maillard network and the accumulation of AGEs concerns the relative contributions of the

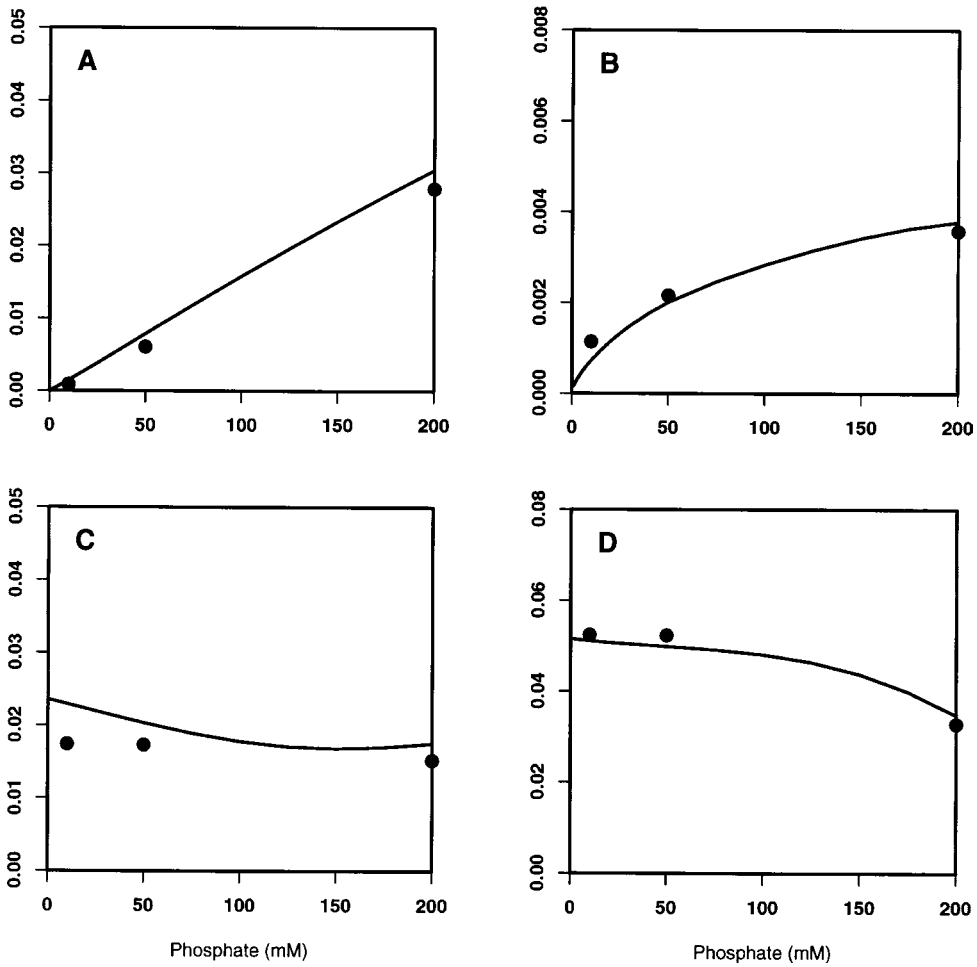


**Figure 5 Double isotope glycoxidation experiments, effect of phosphate concentration**

Experimental (●) and simulated (lines) values at 5 weeks in experiments starting with 100 mM [$^{13}$C]glucose and [$^{12}$C]Amadori product as 0.095 of total lysine as a function of phosphate concentration. Variables, expressed as fraction of total lysine, are (**A**) [$^{13}$C]CML, (**B**) [$^{12}$C]CML, (**C**) [$^{13}$C]Amadori and (**D**) [$^{12}$C]Amadori. Parameters are as in Figure 4, line 2, adjusted according to Table 4.

different pathways to the generation of CML. Insights into the distribution of contributions is a prerequisite for understanding aging processes associated with AGEs and for guiding the development of pharmaceutical products that target the prevention or retardation of degenerative diseases like Alzheimer's that apparently involve AGEs. It is rather difficult to determine the distribution of contributions directly with experimental means. However, given a reliable mathematical model, the contributions can be explored under different conditions. We used for this investigation of the working model specified in Table 5.

Figures 6 and 7 illustrate the distribution of contributions of reactions 4, 5 and 6 to the overall generation of CML as a function of glucose concentrations. Results are presented for two different phosphate concentrations: 200 mM, a concentration used in many experimental conditions, and 10 mM, which is closer to the concentration found *in vivo*. Results are also shown for two different time points, a 1-week (168 h) experiment and a 5-week (840 h) experiment. In addition, we performed simulations of two different scenarios: starting with glucose and non-glycated collagen, a usual design for experiments on glycation and oxidation of proteins *in vitro*, and starting with glucose and collagen that was pre-glycated to its equilibrium level under anti-oxidative conditions. The later scenario intends to mimic *in vivo* conditions where the Amadori product is already present and its level is dependent on glucose concentration.

Our model results suggest that the primary route of CML accumulation involves glyoxal. The dominance of this route is particularly pronounced under glucose concentrations that are close to physiological levels in blood (e.g. 5 mM), which is important because of the constant and direct exposure of extracellular and membrane proteins. This concentration is also similar to intracellular levels in tissues where glucose influx is independent of insulin.

Recalling that the rate constant for glucose autoxidation had to be altered considerably in order to fit the results of $^{12}$C/$^{13}$C competition experiments, we wondered if the glyoxal pathway would still dominate with the original parameter setting. Indeed, simulation results obtained with 50 % of the glucose autoxidation rate constant showed that the glyoxal pathway still accounted for 64 % of CML formation at 5 weeks, for both 5 and 10 mM glucose (details not shown).

Consistent with these findings, Wells-Knecht et al. [19] concluded from the isotope distribution in a $^{12}$C/$^{13}$C competition experiment that the glyoxal route is dominant. However, for low glucose and low phosphate concentrations they assessed the contribution of Amadori oxidation at 50 % of CML generation.

**Table 5 Mathematical description of the kinetic model**

Differential equations

$d[Lys]/dt = \nu_{1b} + f_L \nu_7 - \nu_{1a} - \nu_5$
$d[Schiff]/dt = \nu_{1a} - \nu_{1b} - \nu_{2a} + \nu_{2b} - \nu_6 - \nu_7$
$d[Amadori]/dt = \nu_{2a} - \nu_{2b} - \nu_4$
$d[CML]/dt = \nu_4 + \nu_5 + \nu_6$
$d[Glyoxal]/dt = \nu_3 - \nu_5 - \nu_{5b} + f_L f_G \nu_7$

Rate laws

$\nu_{1a} = p_1\ k_{1a}$ [Glu] [Lys]
$\nu_{1b} = k_{1b}$ [Schiff]
$\nu_{2a} = p_2\ f_{P_i3}\ k_{2a}$ [Schiff]
$\nu_{2b} = p_2\ f_{P_i3}\ k_{2b}$ [Amadori]
$\nu_3 = p_3\ f_{P_i1}\ k_3$ ([Glu]/0.250 M)$^{0.36}$ Ox
$\nu_4 = p_4\ f_{P_i2}\ f_{Glu}\ k_4$ [Amadori] Ox
$\nu_5 = p_5\ k_5$ [glyoxal] [Lys], $\nu_{5b} = k_{5b}$ [glyoxal]
$\nu_6 = p_6\ f_{P_i1}\ k_3$ ([Schiff]/0.250 M)$^{0.4}$ Ox
$\nu_7 = p_7\ f_{P_i1}\ k_3$ ([Schiff]/0.250 M)$^{0.36}$ Ox
$f_{Glu} = 1 + 0.8764\ \{(0.250\ M - [Glu])/0.250\ M\}^{12}$
$f_{P_i1} = ([phosphate]/0.200\ M)^{1.1}$
$f_{P_i2} = ([phosphate]/0.200\ M)^{0.6}$
$f_{P_i3} = 0.57 + 0.43\ ([phosphate]/0.200\ M)^4$

Parameters

$k_{1a} = 0.09\ M^{-1} \cdot h^{-1}$
$k_{1b} = 0.36\ h^{-1}$
$k_{2a} = 0.033\ h^{-1}$
$k_{2b} = 0.0012\ h^{-1}$
$k_3 = p_3\ 7.92 \times 10^{-7}\ M^{-1} \cdot h^{-1}$
$k_4 = 0.000086\ h^{-1}$
$k_5 = 0.019\ M^{-1} \cdot h^{-1}$
$k_{5b} = 0.0017\ h^{-1}$
$f_L = 0.05$
$f_G = 0.1$
$p_1 = 0.11$
$p_2 = 0.75$
$p_3 = 14$
$p_4 = 0.8$
$p_5 = 1$
$p_6 = 1$
$p_7 = 60$
$[Lys]_{TOTAL} = 0.0034$ M
Independent variables are [phosphate] and Ox

This is in contrast to our model predictions, which suggest that the Amadori oxidation pathway is the least and the glyoxal route the most important contributor (Figures 6C, 6D, 7C and 7D). The discrepancy is presumably due to the fact that Wells-Knecht and co-workers obtained their results after pre-glycation with 250 mM glucose, which is much higher than that which a cell would ever experience *in vivo* and therefore biases the conclusions toward the Amadori route. Our simulations assumed an initial Amadori concentration corresponding to equilibrium for a given glucose concentration under anti-oxidative conditions. These values seem to constitute an upper bound for the level of Amadori *in vivo*. Wells-Knecht and collaborators furthermore assumed that all [$^{12}$C]CML was generated through Amadori oxidation, but that might not be realistic. Nevertheless, our model simulations with Amadori compound alone, in total absence of glucose, led after 5 weeks to CML accumulation that was over 70 % due to Amadori oxidation (details not shown).

If the phosphate concentration is high (200 mM), the most important contribution is the formation of CML in the reaction between glyoxal and lysine residues. This dominance is even more significant at low glucose concentrations. Since the generation of CML via glyoxal is a two-stage process, the contribution of this route is more important at later times during the simulations: the relative contribution at 168 h is always less than the contribution at 840 h.

The other two mechanisms, namely the Namiki pathway and the oxidation of the Amadori product, are always lower than the glyoxal route, except for the Amadori product under low phosphate concentration at 168 h and glucose concentrations higher than 20 mM.

**Table 6 Inhibition of CML formation by aminoguanidine (AG)**

CML concentrations at 1 week were simulated under conditions of 200 mM phosphate, using the model in Table 5 with a reaction between glyoxal and aminoguanidine. This reaction was modelled with the rate law proposed by Thornalley and co-workers [33] (first law with respect to both reactants).

| | [CML (fraction of total Lys)] $\times 10^3$ | | | | |
|---|---|---|---|---|---|
| | No AG | | 5 mM AG | | |
| Glucose (mM) | Total | Reaction 5 | Total | Reaction 5 | Inhibition by AG |
| 5 | 0.77 | 0.65 | 0.121 | 0.000318 | 84.3 % |
| 250 | 3.86 | 2.52 | 1.33 | 0.00149 | 65.5 % |
| 42.2 | 1.95 | 1.39 | 0.56 | 0.00072 | 71.3 % |
| 42.2 (with $p_3 = 7$) | 1.26 | 0.70 | 0.57 | 0.000345 | 54.8 % |

### Formation of CML in the presence of aminoguanidine

In line with the investigation of the contributions of different routes to the generation of AGEs it is interesting to assess how the formation of CML is affected by the presence of aminoguanidine, a compound that reacts rapidly with glyoxal and other oxoaldehydes. This compound is often used in model systems for blocking the generation of AGEs via oxoaldehydes, and the interpretation of results is often based on this critical assumption.

We modelled the presence of the inhibiting effect by including an irreversible reaction between glyoxal and aminoguanidine resulting in stable products, assuming mass-action kinetics for the two reactants with a rate constant dependent on phosphate concentrations, as reported in the literature [33]. The formation of CML for three different glucose concentrations in the presence of 5 mM aminoguanidine is shown in Table 6. The simulation results confirm that aminoguanidine is indeed an effective inhibitor of the generation of CML via glyoxal: at the 5 mM concentration, its presence reduces the contribution of this route to negligible levels. As expected, the overall amount of CML generation decreases to values in a range of 15–35 % of the control, since the other two pathways are unaffected by aminoguanidine.

Glomb and Monnier [18] reported AGE formation after 1 week under conditions of only 50 % inhibition by aminoguanidine. They attributed at least 50 % of the CML accumulation to Amadori cleavage, which is much higher than our model predictions. The authors' assessment was based on the assumption that aminoguanidine completely traps glyoxal and blocks the Namiki pathway as well. At least the latter assumption is questionable, however, because it is known that aminoguanidine reacts only with soluble oxoaldehydes. We simulated Glomb and Monnier's conditions, using 42.2 mM glucose, and found at least 71 % inhibition with 5 mM aminoguanidine (Table 6). The discrepancies between Glomb and Monnier's conclusions [18] and

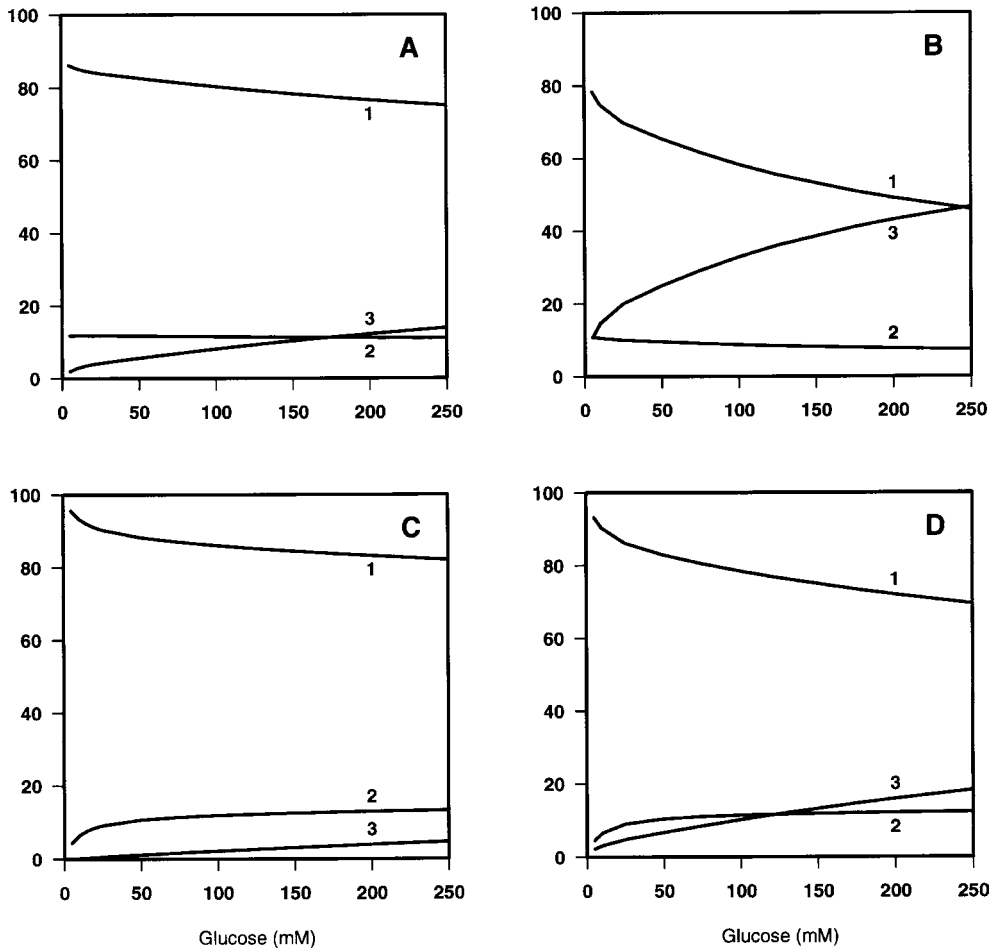


**Figure 6 Contributions to the generation of CML over 840 h**

Values are percentages of the contribution of each reaction (at 840 h) as a function of initial glucose concentration. Phosphate concentrations were 200 mM (**A** and **B**) and 10 mM (**C** and **D**). Contributions are shown for simulations starting with no Amadori product (**A** and **C**) and starting from an initial concentration of Amadori product equal to the equilibrium value obtained under antioxidative conditions (**B** and **D**). Contributions, expressed as percentage of total CML generated, are: lines 1, Glyoxal reaction with lysine (reaction 5); lines 2, Namiki pathway (reaction 6); lines 3, oxidative cleavage of Amadori product (reaction 4).

our model results may be due to the fact that the generated amount of CML is very sensitive to the rate of glucose autoxidation, which in turn is very sensitive to the oxidative conditions of the experiments, as determined by trace amounts of metals, the presence of chelators, and so forth. It is unclear to what degree Glomb and Monnier's conditions were directly comparable with ours. With the parameter settings given here, the model predicted twice the amount of CML after 1 week, but if the corresponding adjustment factor $p_3$ was halved, the model agreed with Glomb and Monnier's data, since only 55% inhibition is observed (see Table 6). This indicates, first, that some model parameters are sensitive and have a strong effect on the model dynamics and, secondly, that even rather different experimental conditions still fall within the realm of responses that can be captured with the model. It should be noted that the amounts of generated CML vary considerably among the different experimental groups and even between different papers from the same laboratory. For instance, the amount of CML at 5 weeks reported by Wells-Knecht et al. [19] is twice that reported by Fu et al. [12].

Glomb and Monnier [18] proposed an additional mechanism for the generation of CML through the Namiki pathway, postulating the release of glyoxal in an oxidation starting with the Schiff base. Our model implicitly accounts for such a mechanism in reaction 7. The flux through this reaction is an upper boundary for the generation of glyoxal from the Schiff base, and comparisons of the contributions of glucose autoxidation and Namiki pathway imply that the former accounts for more than 98% of glyoxal generation over a wide range of glucose and phosphate concentrations.

One should mention a conclusion from the model that is at odds with the general belief that the presence of protein significantly increases the generation of glyoxal. If the Namiki pathway is accounted for as a second source of glyoxal, the model implies that glucose autoxidation is as strongly responsible for glyoxal formation as the elevated availability of protein. The discrepancy in importance of autoxidation between current understanding and model prediction may be related to the fact that accounting for elevated protein levels in the modified model required us to increase the rate parameter for autoxidation in reaction 3 by an order of magnitude over the rate that was initially proposed for this reaction in the absence of protein. Our model does not provide a mechanistic explanation for the necessary increase. However, our findings are consistent with the fact that oxidative stress and the Maillard reaction are not independent of each other. Specifically,

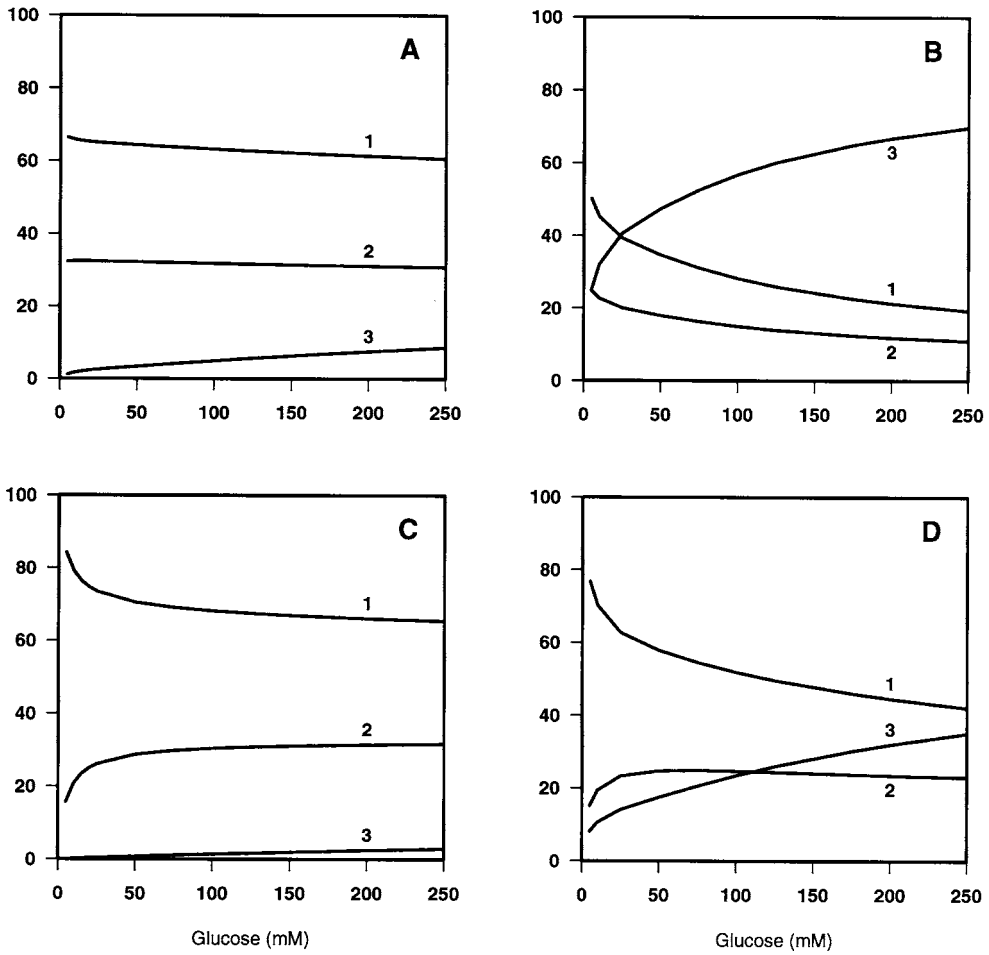


**Figure 7 Contributions to the generation of CML over 168 h**

Values are percentages of the contribution of each reaction (at 168 h) as a function of initial glucose concentration. All other details are as for Figure 6.

it is known that oxidative stress is enhanced in glycoxidation experiments and in turn influences glucose autoxidation, which may explain our model results to some degree.

## Conclusion

In comparison with glycolysis and the pentose phosphate pathway, the amount of glucose entering the Maillard reaction is negligible. Only minute amounts of glucose are oxidized to glyoxal or form a Schiff base with lysine, and it is tempting to ignore these fates altogether. However, some of these intermediates ultimately become AGEs, and their life-long accumulation and extremely slow degradation contribute to degenerative diseases that become ever more important in an aging society.

Information about the Maillard reaction network is distributed throughout the biochemical literature in bits and pieces. This makes it difficult to comprehend the short-term dynamics of glyoxal, Schiff bases and Amadori compounds on a time scale of hours and to predict the consequences of small changes in the AGE dynamics on a longer time scale of years and decades. The model presented here is an attempt to integrate the available information into a functioning entity that can be queried on both time scales.

The construction of the model occurred in two phases. First, local kinetic information was collected and entered into rate laws describing the dynamics of the key components of the Maillard system. While the immediate result was not optimal, this assemblage of diverse raw data yielded a reference model that already performed relatively well, supporting the general experience that model structure typically determines responses more strongly than precise parameter values.

The parameters of the reference model were either estimated directly from quantitative kinetic measurements or deduced indirectly from quantitative or qualitative relationships among metabolites. As a consequence, these point estimates differed quite widely in quality and reliability. Some parameters were identified rather robustly, while others could only be assumed to fall within one or two orders of magnitude of the chosen reference value.

In order to restrict these uncertainties and to constrain the behaviour of the model, the parameters were subjected to a second phase of adjustment that used data of a different nature. They consisted of global observations about the Maillard system, either in the form of long-term responses to perturbed conditions or of time series measurements, showing the temporal developments of key metabolites. Analysis of these types of data allowed us to adjust the model parameters such that the overall dynamic model appeared to capture all observations well, including those at slow and fast time scales, different oxidative states, and measurements made under different conditions of glucose and phosphate availability.

The chosen model structure consists primarily of elemental chemical kinetics in the form of mass-action rate laws. This was assumed to be appropriate because many of the involved steps are spontaneous and independent of the action of enzymes. In some cases, however, reaction steps actually consist of multiple processes or are enzyme-catalysed, and this necessitated other types of rate descriptions. As a direct extension of mass-action laws, we selected power functions for this purpose. These allow kinetic orders to be non-integer and therefore are more flexible in modelling exponential or hyperbolic rates. They are also guaranteed by Taylor's well-known theorem of numerical analysis to be valid approximations of rates that are not originally in power-law form.

As an example of the quality of the power-law representation, consider the long-term dependence of [$^{13}$C]CML on [$^{13}$C]glucose substrate, as shown in Figures 3(A) and 4(A). Because the glyoxal route dominates the generation of CML under the given conditions, the total accumulation of CML at a particular time point (here at 5 weeks) is strongly influenced by the rate of reaction 3 (Table 1) and will follow this rate if glucose consumption is negligible and glyoxal is in quasi-steady state. Reaction 3, the autoxidation of glucose, is a process that actually consists of an entire network of reactions. Even though each individual step is non-enzymic and presumably well represented by mass-action kinetics, one must expect that the overall response of the reaction network will be non-linear and deviate from mass action. As a well-known example of such a switch from mass action to a different type of non-linear kinetics, consider the Michaelis–Menten reaction, which constitutes a simple 'system' of elemental reactions but overall exhibits characteristics that differ from one individual mass-action step. In the case of glucose autoxidation, the dependence of the rate on glucose concentration is apparently well captured by a power-law function. This functional form is directly supported by experimental measurements of the final resulting product, [$^{13}$C]CML, and fits the data better than, for instance, a hyperbolic function of Michaelis–Menten type (Figure 8). Although originally derived from local data, the assumption of a power-law rate for this process in our model is therefore consistent with global results.

With its combination of elemental mass-action and generalized power-law rates, the fully adjusted model (Table 5) appears to capture the short- and long-term dynamics of the Maillard reaction and the accumulation of CML rather well. It is consistent with kinetic data on individual reaction steps, produces observed time dynamics over comparably long time spans, and captures validly the dependence of the system on glucose and phosphate availability.

Like any abstraction, the model is dependent on assumptions that may have to be investigated further in future work. For instance, we assume that CML is a valid representative of all AGE formation and ignore other AGEs. Similarly, the model does not account for non-oxidative formation of AGE via 3-deoxyglucosone from Amadori compounds [30,34] and via sugars smaller than glucose, in particular arabinose, which is formed during glucose autoxidation and can cross-link proteins non-oxidatively [17,35].

The model emphasizes the importance of glyoxal as an intermediate in the generation of CML. Other 2-oxoaldehydes like methylglyoxal and 3-deoxyglucosone are also known to promote fast browning and cross-linking in proteins *in vitro* [30] and may be important intermediates in the Maillard reaction *in vivo*. For more detailed studies of diabetic consequences of AGE accumulation, it might be useful to extend the present focus to 2-oxoaldehyde scavengers, like aminoguanidine, which appear to be promising treatment agents against diabetic complications. Such theoretical studies could complement experimental investigations of naturally occurring compounds that specifically react with 2-oxoaldehydes.

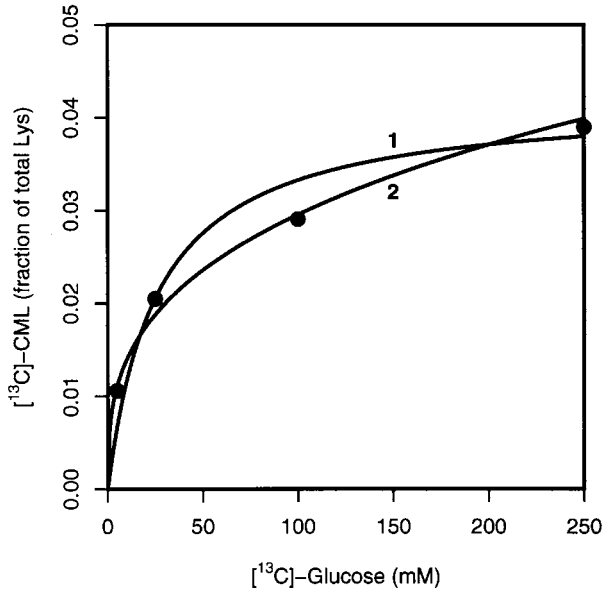


**Figure 8 Dependence of the accumulation of [$^{13}$C]CML in double-isotope glycoxidation experiments**

Experimental data (●) and least-squares fits (lines) with a power-law function (line 1) and a Michaelis–Menten rate function (line 2). Data represent [$^{13}$C]CML at 5 weeks in experiments starting with [$^{13}$C]glucose and [$^{12}$C]Amadori product as 0.095 of total lysine.

Of course, the model is primarily based on data obtained *in vitro*, and any extrapolations from our simulation results towards normal functioning *in vivo* or a disease state must occur with adequate caution. For instance, the model predicts the dominance of the glyoxal route in the generation of CML, but these predictions are based on the chemical dynamics in closed *in vitro* experiments of collagen glycation by glucose. Evaluations that are closer to the natural physiology of living organisms will require several model extensions and significant future research. As a particularly important example for such an extension, the glyoxalase system provides a physiological defence mechanism against AGE formation that acts synergistically with glutathione. Thus, a first natural model extension will be the inclusion of glutathione. This particular metabolite and its interactions with the glyoxylase network will be discussed in a forthcoming paper, along with the effects of protein turnover.

A. E. N. F. acknowledges Fundação Luso-Americana para o Desenvolvimento for support. This work was supported in part by a Quantitative Systems Biotechnology grant (BES-0120288; to E. O. V.) from the National Science Foundation. Any opinions, findings and conclusions or recommendations expressed in this material are those of the authors and do not necessarily reflect the views of the sponsoring institutions.

## REFERENCES

1 Sell, D. R., Lane, M. A., Johnson, W. A., Masoro, E. J., Mock, O. B., Reiser, K. M., Fogarty, J. F., Cutler, R. G., Ingram, D. K., Roth, G. S. and Monnier, V. M. (1996) Longevity and the genetic determination of collagen glycoxidation kinetics in mammalian senescence. Proc. Natl. Acad. Sci. U.S.A. **93**, 485–490

2 Sell, D. R., Lapolla, A., Odetti, P., Fogarty, J. and Monnier, V. M. (1992) Pentosidine formation in skin correlates with severity of complications in individuals with long-standing IDDM. Diabetes **41**, 1286–1292

3 Dyer, D. G., Dunn, J. A., Thorpe, S. R., Bailie, K. E., Lyons, T. J., McCance, D. R. and Baynes, J. W. (1993) Accumulation of Maillard reaction products in skin collagen in diabetes and aging. J. Clin. Invest. **91**, 2463–2469

4 Colaco, C., Ledesma, M. D., Harrington, C. R. and Avila, J. (1996) The role of the Maillard reaction in other pathologies: Alzheimer's disease. Nephrol. Dial. Transplant. **11**, suppl. 5, 7–12

5 Vlassara, H. and Palace, M. R. (2002) Diabetes and advanced glycation endproducts. J. Intern. Med. **251**, 87–101

6 Colaco, C. (ed.) (1997) The Glycation Hypothesis of Atherosclerosis, Landes Bioscience, Austin, TX

7 Münch, G., Schinzel, R., Loske, C., Wong, A., Durany, N., Li, J. J., Vlassara, H., Smith, M. A., Perry, G. and Riederer, P. (1998) Alzheimer's disease–synergistic effects of glucose deficit, oxidative stress and advanced glycation endproducts. J. Neural Transm. **105** 439–461

8 Edelstein, D. and Brownlee, M. (1992) Mechanistic studies of advanced glycosylation end product inhibition by aminoguanidine. Diabetes **41**, 26–29

9 Shoda, H., Miyata, S., Liu, B. F., Yamada, H., Ohara, T., Suzuki, K., Oimomi, M. and Kasuga, M. (1997) Inhibitory effects of tenilsetam on the Maillard reaction. Endocrinology **138**, 1886–1892

10 Khalifah, R. G., Baynes, J. W. and Hudson, B. G. (1999) Amadorins: novel post-Amadori inhibitors of advanced glycation reactions. Biochem. Biophys. Res. Commun. **257**, 251–258

11 Ruggiero-Lopez, D., Lecomte, M., Moinet, G., Patereau, G., Lagarde, M. and Wiernsperger, N. (1999) Reaction of metformin with dicarbonyl compounds. Possible implication in the inhibition of advanced glycation end product formation. Biochem. Pharmacol. **58**, 1765–1773

12 Fu, M., Wells-Knecht, K. J., Blackledge, J. A., Lyons, T. J., Thorpe, S. R. and Baynes, J. W. (1994) Glycation, glycoxidation and cross-linking of collagen by glucose. Diabetes **43**, 676–683

13 Ahmed, M. U., Frye, E. B., Degenhardt, T. P., Thorpe, S. R. and Baynes, J. W. (1997) $N^{\varepsilon}$-(carboxyethyl)lysine, a product of the chemical modification of proteins by methylglyoxal, increases with age in human lens proteins. Biochem. J. **324**, 565–570

14 Reddy, S., Bichler, J., Wells-Knecht, K. J., Thorpe, S. R. and Baynes, J. W. (1995) $N^{\varepsilon}$-(carboxymethyl)lysine is a dominant advanced glycation endproduct (AGE) antigen in tissue proteins. Biochemistry **34**, 10872–10878

15 Ahmed, M. U., Thorpe, S. R. and Baynes, J. W. (1986) Identification of $N^{\varepsilon}$-(carboxymethyl)lysine as a degradation product of fructoselysine in glycated protein. J. Biol. Chem. **261**, 4889–4894

16 Wolff, S. P. and Dean, R. T. (1987) Glucose autoxidation and protein modification. Biochem. J. **245**, 243–250

17 Wells-Knecht, K. J., Zyzak, D. V., Lichfield, J. E., Thorpe, S. R. and Baynes, J. W. (1995) Mechanism of autoxidative glycosylation: identification of glyoxal and arabinose as intermediates in the autoxidative modification of proteins by glucose. Biochemistry **34**, 3702–3709

18 Glomb, M. A. and Monnier, V. M. (1995) Mechanism of protein modification by glyoxal and glycolaldehyde, reactive intermediates of the Maillard reation. J. Biol. Chem. **270**, 10017–10026

19 Wells-Knecht, M. C., Thorpe, S. R. and Baynes, J. W. (1995) Pathways of formation of glycoxidation products during glycation of collagen. Biochemistry **34**, 15134–15141

20 Maillard, L. C. (1912) Action des acides aminés sur les sucres: formation des mélanoidines par voie méthodique. C. R. Acad. Seances Paris **154**, 66–68

21 Savageau, M. A. (1969) Biochemical Systems Analysis, I. Some mathematical properties of the rate law for the component enzymatic reactions. J. Theor. Biol. **25**, 365–369

22 Savageau, M. A. (1969) Biochemical Systems Analysis, II. The steady-state solutions for an n-pool system using a power-law approximation. J. Theor. Biol. **25**, 370–379

23 Voit, E. O. (2000) Computational Analysis of Biochemical Systems, Cambridge University Press, Cambridge

24 Torres, N. V. and Voit, E. O. (2002) Pathway Analysis and Optimization in Metabolic Engineering, Cambridge University Press, Cambridge

25 Baynes, J. W., Thorpe, S. R. and Murtiashaw, M. H. (1984) Nonenzymatic glucosylation of lysine residues in albumin. Methods Enzymol. **106**, 88–98

26 Shapiro, R., McManus, M. J., Zalut, C. and Bunn, H. F. (1980) Sites of nonenzymatic glycosylation of human hemoglobin A. J. Biol. Chem. **255**, 3120–3127

27 Watkins, N. G., Thorpe, S. R. and Baynes, J. W. (1985) Glycation of amino groups in protein. J. Biol. Chem. **260**, 10629–10636

28 Smith, P. R. and Thornalley, P. J. (1992) Mechanism of the degradation of non-enzymatically glycated proteins under physiological conditions. Eur. J. Biochem. **210**, 729–739

29 Zyzak, D. V., Richardson, J. M., Thorpe, S. R. and Baynes, J. W. (1995) Formation of reactive intermediates from Amadori compounds under physiological conditions. Arch. Biochem. Bioophys. **316**, 547–554

30 Westwood, M. E. and Thornalley, P. J. (1997) Glycation and advanced glycation endproducts. In The Glycation Hypothesis of Atherosclerosis (Colaco, C., ed.), pp. 57–87, Landes Bioscience, Austin, TX

31 Thornalley, P. J., Wolff, S., Crabbe, J. and Stern, A. (1984) The autoxidation of glyceraldehyde and other monosaccharides under physiological conditions catalysed by buffer ions. Biochim. Biophys. Acta **797**, 276–287

32 Watkins, N. G., Neglia-Fisher, C. I., Dyer, D. G., Thorpe, S. R. and Baynes, J. W. (1987) Effect of phosphate on the kinetics and specificity of glycation of protein. J. Biol. Chem. **262**, 7207–7212

33 Thornalley, P. J., Yurek-George, A. and Argirov, O. K. (2000) Kinetics and mechanism of the reaction of aminoguanidine with the a-oxoaldehydes glyoxal, mehylglyoxal, and 3-doxyglucosone under physiological conditions. Biochem. Pharmacol. **60**, 55–65

34 Kato, H., Shin, D. B. and Hayase, F. (1987) 3-Deoxyglucosone crosslinks proteins under physiological conditions. Agric. Biol. Chem. **51**, 2009–2011

35 Litchfield, J. E., Thorpe, S. R. and Baynes, J. W. (1999) Oxygen is not required for the browning and crosslinking of protein by pentoses: relevance to the Maillard reactions *in vivo*. Int. J. Biochem. Cell Biol. **31**, 1297–1305

36 Iberg, N. and Flückiger, R. (1986) Nonenzymatic glycosylation of albumin *in vivo*. J. Biol. Chem. **261**, 13542–13545


Received 2 April 2003/4 August 2003; accepted 11 August 2003
Published as BJ Immediate Publication 11 August 2003, DOI 10.1042/BJ20030496